Air-coupled ultrasound as an accurate and reproducible method for bonding assessment of glued timber

Author(s):
Sanabria, Sergio J.; Mueller, Christian; Neuenschwander, Jürg; Niemz, Peter; Sennhauser, Urs

ORIGINAL

Air-coupled ultrasound as an accurate and reproducible method for bonding assessment of glued timber

**Sergio J. Sanabria · Christian Mueller ·
Juerg Neuenschwander · Peter Niemz ·
Urs Sennhauser**

Abstract Glued timber products are widely used in construction; therefore, it is necessary to develop non-destructive bonding quality assessment methods for long-term structural health monitoring. Air-coupled ultrasound (ACU) inspection is a novel technique, with phenomenal improvements in reproducibility compared to traditional contact ultrasonics, unlimited scanning possibilities, and a high potential for delamination detection in wood products. As part of an ongoing project, glued timber samples of 10 mm thickness with artificial glue line defects were inspected. A normal through-transmission set-up with 120 kHz transducers allowed for successful and accurate imaging of the geometry of glued and non-glued areas in all inspected objects. The influence of wood heterogeneity and the reproducibility of ACU amplitude measurements were analysed in detail, identifying the main sources of variation. Future work is planned for the inspection of more complex glued timber objects.

Introduction

Glued solid wood products have gained much importance over recent years, as they allow an efficient and versatile use of the renewable timber material. Quality monitoring is necessary during production but also during use in order to prevent security hazards and to decide what restoration works are required. Among others, the integrity and load bearing capacity of the glue line need to be tested. During

S. J. Sanabria (✉) · J. Neuenschwander · U. Sennhauser
Electronics/Metrology/Reliability Laboratory, Swiss Federal Laboratories for Materials Science
and Technology, Empa, Ueberlandstrasse 129, 8600 Duebendorf, Switzerland
e-mail: sergio.sanabria@empa.ch

C. Mueller · P. Niemz
Laboratory for Wood Physics and Non-Destructive Testing Methods, Institute for Building
Materials, ETH Zurich, Schafmattstrasse 6, 8093 Zurich, Switzerland

fabrication, inadequate environmental conditions and curing times can lead to glue line defects; in-service fluctuations of temperature and air humidity and long-term sustained loads induce cracking and delaminations in the glue line (Dunky and Niemz 2002).

Current European standardised methods of assessing bonding quality involve destructive tests performed on a small percentage of samples from the total production. They consist of a combination of climatic cycling, visual inspection of the glue line (EN 391:2001) and mechanical tests (e.g. shear, tensile and bending strength, creep behaviour; EN 14080:2005). Acoustical techniques are irreplaceable tools for the non-destructive evaluation of adhesive-bonded composites, due to their high sensitivity to adhesion defects and the possibility to inspect real size structures during use (Maeva et al. 2004). An X-ray tomography system with 0.25 mm resolution has also been successfully applied to determine the bonding quality of finger joints (Hu and Gagnon 2007).

Ultrasonic discrete point measurements in contact technique (transducers pressed onto the sample, either directly or with a thin intermediate acoustic matching layer) have traditionally been used, since they allow coupling of sufficient acoustic energy to penetrate large glued timber objects (Hasenstab 2006). Dry coupling (e.g. with an elastomeric material or no coupling agent) is generally preferred to coupling agents such as gel, grease, liquid, etc. which may penetrate the wood surface altering the acoustic properties of the product and contaminating it. A main drawback is that amplitude measurements show poor reproducibility; Aicher et al. (2002) reported voltage uncertainty values of 20–25% for a transducer coupled without agent by hand pressure to glued laminated timber; variations of coupling pressure have a strong effect on repeatability and the waviness of wood surfaces may introduce misalignment errors between transducers and sample. Large glue line defects in glued timber structures have been detected with contact technique using longitudinal wave through-transmission (Dill-Langer et al. 2005a) and shear wave reflection measurements (Dill-Langer et al. 2005b). Biernacki and Beall (1996) used a through-transmission set-up at normal and angular (5°) incidence to monitor the curing phases of sound and defective bonds (e.g. kissing bonds and slip bonds); the transducers were glued to the specimen with hot-melt adhesive. Better repeatability of the ultrasonic amplitude (variations smaller than 5%) and one-dimensional continuous scanning is achieved with roller transducers, which have been applied to defect inspection in hardwood lumber (Kabir et al. 2002).

Hybrid inspection methods couple high-power ultrasound into the sample with a welding transducer and record the ultrasonic wave interactions in the glue line with a non-contact non-ultrasonic method. Solodov et al. (2004) have assessed delaminations between veneer lamina and particle board scanning the sample with a laser vibrometer and performing non-linear analysis of the waveforms. Choi et al. (2008) used an infrared camera in order to detect temperature changes due to the interaction of high-power ultrasound with delamination defects located at a depth of 10 mm from the surface of a glued timber sample.

Air-coupled ultrasonics (ACU) is a novel inspection technique that provides practically unlimited scanning resolution in any direction and very high reproducibility, since the transducers can be moved at a certain distance from the surface of

the object. The main drawback is the small coupling of acoustic energy into the sample; however, this problem has been overcome in recent years with new transducer technologies (Kunkle et al. 2006). High-power low-frequency ACU systems for split detection in wood composites are currently used in production lines [UPU 5000, Fagus-GreCon Greten GmbH & Co. KG, Alfeld, Germany; Ultra-Scan 40+, Electronic Wood Systems Int., Beaverton, OR, USA; see also Niemz and Sander (1990)]. Ultrasonic imaging has been performed in through-transmission mode to image missing glue in a wood veneer sample (Stoessel 2004) and for inspection of density, knots, microcracks and drilled holes in solid wood (Gan et al. 2005; Hasenstab et al. 2005). Delaminations in wood panel paintings, between solid wood and a thin plaster layer, have been assessed with both normal through-transmission and single-sided inspection (Siddiolo et al. 2007).

In this work, the application of ACU to assess lack of adhesive in glued solid wood objects is demonstrated. A longitudinal normal through-transmission measurement set-up and data evaluation based on voltage level measurements of recorded A-scans allow for the precise imaging of areas with and without adhesive due to the different acoustic impedance of the glue line in each case. The impact of the heterogeneity of wood structure in the amplitude measurements and the reproducibility of the ACU technique identifying the main sources of variation are analysed.

Materials and methods

Sample preparation

A total of 46 samples of common spruce (*Picea abies* Karst.) were manufactured in the Laboratory for Wood Physics at ETH Zurich; each consisting either of a 10-mm thick solid wood board or two 5-mm thick solid wood lamellas glued together except for some defined areas (Table 1). The adhesive is a one-component moisture-curing polyurethane resin (HB 110, Purbond AG, Sempach Station, Switzerland) applied to one side of the lamellas with an amount of 200 g m^{-2}. The lamellas were pressed together in a hydraulic press for 3 h with a pressure of 0.8 N mm^{-2}. Prior to gluing, the wood was conditioned to normalised climatic conditions ($T = 20°C$ and RH = 65%), which were also used for storage afterwards.

Only solid wood lamellas with a small percentage of knots, resin pockets, grain distortion, etc. were used in order to analyse the variability of ultrasonic signals

Table 1 Description of glued timber samples manufactured for ACU measurement

Type	Description
A	Single solid wood lamella of dimensions 500 × 100 × 10 mm^3
B	Two lamellas of dimensions 500 × 100 × 5 mm^3 glued together to form a glued timber beam of 500 × 100 × 10 mm^3
C	Same geometry as B. No adhesive applied in the left half area (250 × 100 mm^2) of the beam
D	Same geometry as B. Adhesive only applied in two small areas (about 30 × 100 mm^2) on the left and right edges of the beam

propagating through defect-free glued timber. The cross-section of the samples is approximately in the orthotropic R-T plane, the ring angle varying between 90° (T direction) and 45°. The curvature of the year rings is negligible. An aluminium sheet of 1 mm thickness was introduced in the edge of samples of type C to control the air gap between non-glued lamellas. After ultrasonic measurement, samples of type C were broken up and the profile of the transition between glued and non-glued areas was highlighted with a pencil and recorded with optical means.

Theoretical considerations

The interpretation of the measurements is based on plane wave theory for homogeneous isotropic layered media (Brekhovskikh 1980). The sample is modelled as a three layer system, i.e. wood/glue/wood for glued material and wood/air/wood in the case of non-glued material. Due to the high acoustic impedance mismatch between air and solids, the pressure level of an ACU signal that propagates through non-glued material is significantly lower than in the case of glued material, since most of the acoustic energy is reflected at the wood–air interfaces. Only a single echo of a longitudinal wave propagating through the three layers is considered. The acoustic attenuation in the glue line is neglected. It is assumed that the voltage level measured with an ACU transducer is proportional to the force exerted on its surface by ultrasonic waves (Schmerr and Song 2007).

The amplitude level ratio between ACU signals propagating through glued and non-glued material $L_{\text{glued/non-glued}}$ (dB) can be calculated as follows:

$$L_{\text{glued/non-glued}} = 20 \log_{10} \frac{V_{\text{glued}}}{V_{\text{non-glued}}} = T_{\text{wood,glue,wood}} - T_{\text{wood,air,wood}}$$

$$T_{1,2,1} = 20 \log_{10} \left[\frac{4Z_1 Z_2}{(Z_1 + Z_2)^2} \right] \quad Z_i = \rho_i c_i \tag{1}$$

V_{glued} (V) and $V_{\text{non-glued}}$ (V) are the corresponding voltage measurements in the recorded A-scans. $T_{1,2,1}$ (dB) is the transmission coefficient for a single echo propagating through a layer of material 2 between two semi-infinite media of material 1. $Z_i (\text{Pa s m}^{-1})$, $\rho_i (\text{kg m}^{-3})$ and $c_i (\text{m s}^{-1})$ are the acoustic impedance, density and speed of sound in the propagation direction for medium i, respectively. The average speed of sound in the samples $c_{\text{spruce}} = 1,300 \, \text{m s}^{-1}$ was measured following a similar method to the one by Vun et al. (2003), as well as the average density with gravimetrical determination $\rho_{\text{spruce}} = 409 \, \text{kg m}^{-3}$; therefore, $Z_{\text{wood}} = 0.532 \times 10^6 \, \text{Pa s m}^{-1}$. From literature data (Deutsch et al. 1997) $Z_{\text{glue}} = 2.2 \times 10^6 \, \text{Pa s m}^{-1}$ (polyurethane) and $Z_{\text{air}} = 0.000427 \times 10^6 \, \text{Pa s m}^{-1}$ (dry air $T = 20°C$). From Eq. 1 it follows that $T_{\text{wood,glue,wood}} = -4.1 \, \text{dB}$ and $T_{\text{wood,air,wood}} = -49.9 \, \text{dB}$.

Experimental set-up

The measurement set-up is shown in Figs. 1 and 2. Two ACU broadband planar transducers are aligned perpendicularly to the surfaces of the sample, one transmitting an ultrasonic signal and the other one receiving it. The transducers
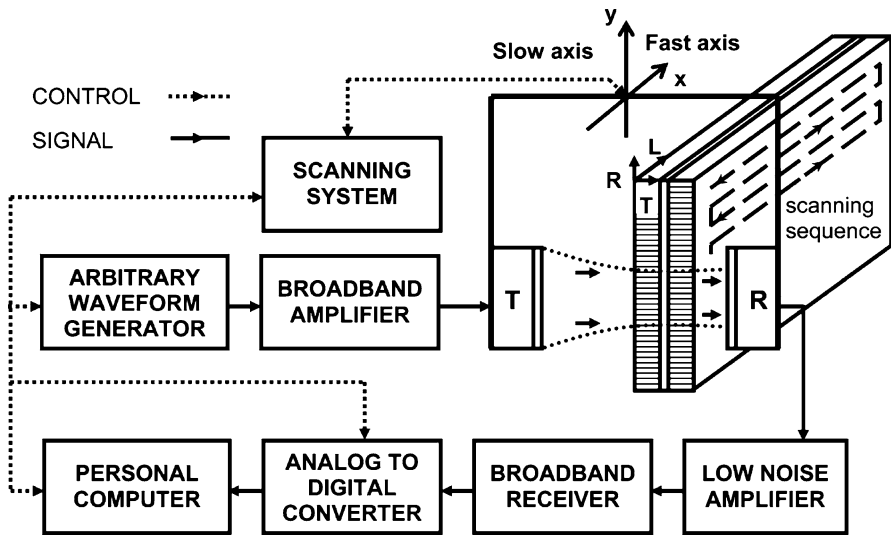
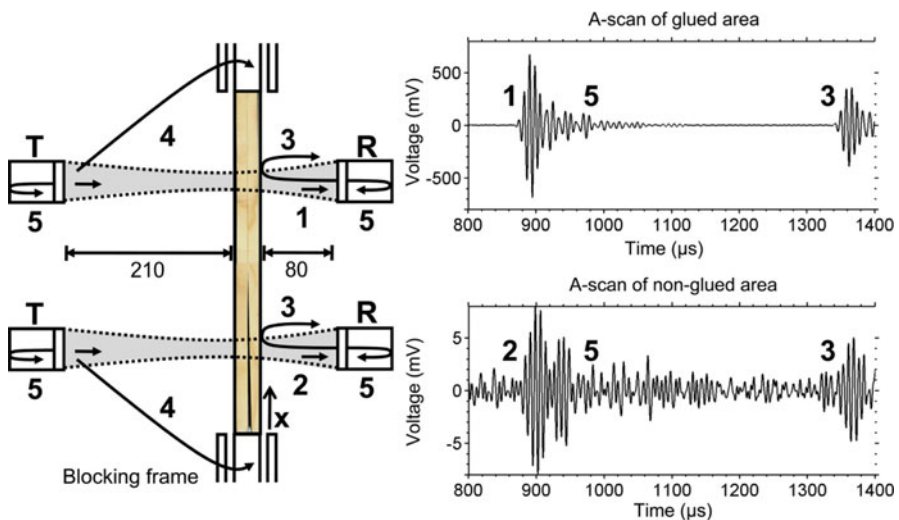**Fig. 1** ACU measurement set-up and block diagram of equipment

Fig. 2 Main propagation paths and typical A-scans. *1* and *2* are waves propagating through the sample. *3* are multiple reflections between receiver and sample. *4* are waves blocked by the frame built around the object. *5* are multiple reflections in the damping mass of the transducers

are Gas Matrix Piezoelectric Composites (NCG100-D50, The Ultran Group Inc., State College, PA, USA) with a central frequency of 120 kHz and 50-mm active diameter (Kunkle et al. 2006). The distance between the transmitter and the sample was chosen to achieve a nearly planar sound field with minimum beam width, according to the measurements performed by Hasenstab et al. (2005). A three-axis

system (ISEL Germany AG, Eichenzell) moves the two transducers together as a fixed unit; scanning the surface of the samples with steps of 1 mm in the fast axis and 4 mm in the slow axis. The glued timber samples are introduced into a fixation frame that allows for reproducible alignment with the insonification axis. A 100 MS/s 16 bit arbitrary waveform generator (NI PCI-5421, National Instruments Corp., Austin, TX, USA) generates a 33 µs length 120 kHz sinusoidal pulse windowed with a Gaussian function, which is amplified to 115 Vpp amplitude with a broadband unit (75A250, Amplifier Research Corp., Souderton, PA, USA) and fed into the transmitter transducer. Received ultrasonic signals are filtered and amplified 52 dB with a low-noise preamplifier (5660C, Olympus NDT Inc., Waltham, MA, USA) and a broadband receiver (BR-640A, RITEC Inc., Warwick, RI, USA), both specified for ultrasonic applications. The voltage waveforms are then digitised by means of a data acquisition board (NI PCI-5122) with a sampling frequency of 2.5 MHz and 14 bits resolution, the generated A-scans being stored for each scanned position x, y. The equipment is controlled with a modified version of a LabVIEW® (NI) software previously used for immersion technique measurements (Gattiker et al. 2007).

The recorded A-scans were evaluated with self-developed software based on Matlab® (2008a, The MathWorks Inc., Natick, MA, USA). A digital 50 kHz/250 kHz band-pass filter reduced the noise level to 0.8 mV$_{rms}$. This value corresponds to the quantification noise of the NI PCI-5122. C-scans were generated from a peak or root mean square (rms) voltage measurement for each A-scan and a defined time gate $\mathbf{T_{gate}}$:

$$V_{peak} = \max_{\mathbf{T_{gate}}} V(t) \quad \mathbf{T_{gate}} = [t_1, t_2]$$

$$V_{rms} = \sqrt{\frac{1}{t_2 - t_1} \int_{t_1}^{t_2} V(t)^2 dt} \tag{2}$$

Results and discussion

Figure 2 shows two A-scans recorded through glued and non-glued wood with the same equipment settings and without averaging; the main propagation paths are indicated. The distance between receiver and sample allows for separating in time multiple reflections between their surfaces (3) from measured waves (1) and (2). Waves recorded through bonded material (1) present a signal-to-noise ratio of 60 dB, which allows for enough dynamic range to record signals from glued and non-glued areas without changing the equipment settings. On the other hand, the transducers show poor damping performance (5); the received pulses are about three times longer (120 µs for a 20 dB level reduction) than the ones excited into the transmitter probe. Ultrasonic signals recorded through non-glued wood (2) show a high voltage level reduction and a strong pulse shape distortion with respect to glued areas, both of which are dependent on the air gap thickness between the lamellas. Waves diffracted at the edges of the sample (4) are blocked by the fixation frame
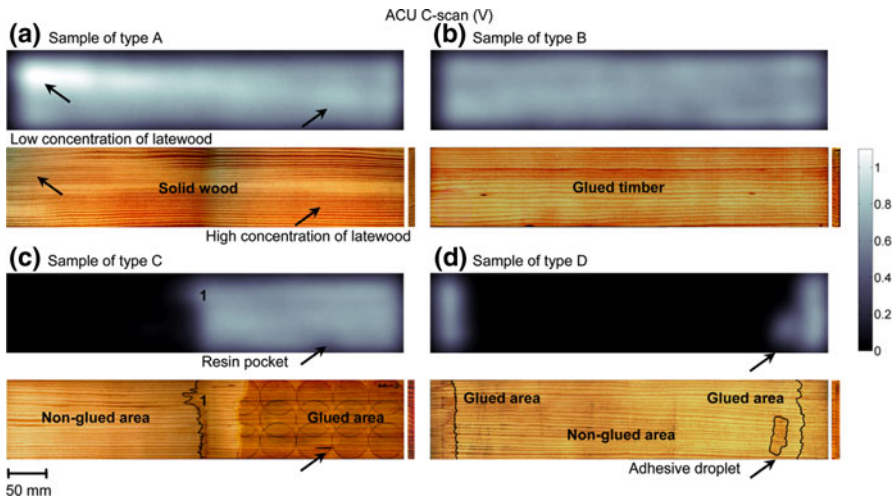
Fig. 3 ACU imaging (*top* **a**, **b**, **c** and **d**) and photographs (*bottom* **a**, **b**, **c** and **d**) of glued timber objects. The photographs of samples of types A and B correspond to the beam external surfaces; the ones of samples of types C and D to the glue line plane

built around the inspected object. The frame is made from wood (Norway spruce) covered by several layers of paper with small air gaps in between. Waves propagating through the frame are strongly attenuated due to the accumulation of impedance mismatch losses.

ACU imaging of glue presence

Figure 3 demonstrates successful ultrasonic imaging of absence and presence of adhesive. Typical C-scans for samples of types A, B, C and D are presented. A quasi-homogenous amplitude level is observed for samples of types A and B. As expected, the ultrasonic signal shows a clear decrease in amplitude in the non-glued region of samples of type C and D. Details of the transition between glued and non-glued areas down to 20 mm diameter can be resolved and correlated with the photographs of the open lamellas; for example, feature 1 in Fig. 3c or an adhesive droplet in Fig. 3d. Best resolution performance is achieved with the shortest time gates (in the C-scans a peak measurement with a time gate of 860–895 μs was used, see waveform in Fig. 4). A possible reason for this improvement is that secondary wave propagation paths are partially filtered out, such as ultrasonic energy bypassing via the bonded region. Peak and rms voltage measurements give similar results for short time gates. The main resolution limiting factor is the spatial smearing introduced by the sound field radiated by the planar ACU transducers. Further improvement in resolution might be achieved using focused transducers or deconvolution image processing (Rangarajan et al. 2008). The authors are currently developing deconvolution algorithms for glued timber assessment.

Figure 4 shows a typical voltage profile along the fast axis for a typical C-sample normalised to the signal level received through glued material; a peak measurement
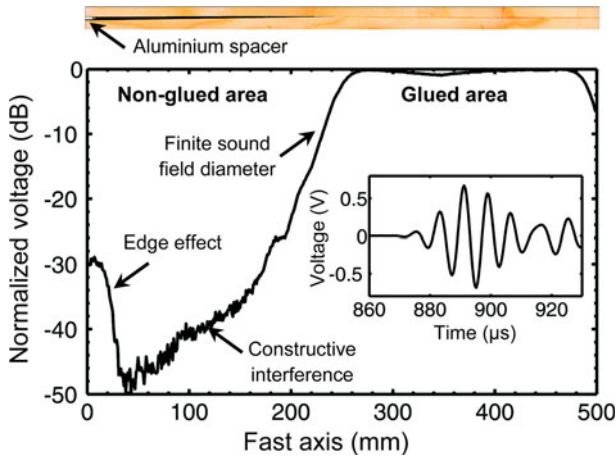
Fig. 4 Profile of peak voltage level for a typical C-sample measured with a time gate of 860–930 μs; a gated A-scan is also shown

with a time gate of 860–930 μs was used. The gap thickness between both lamellas was measured optically and decreased linearly from 1 mm at the position of the aluminium sheet to less than 100 μm in the transition to bonded material. The normalised voltage level shows a minimum of −50 dB, in good agreement with the estimation for $T_{wood,air,wood}$ given by Eq. 1. As the air gap thickness between lamellas decreases, the voltage level rises, owing to constructive interference within the gap of multiple reflections of the ultrasonic wave (a detailed theoretical analysis of these variations will be published elsewhere). About 20 mm from the transition to the glued area, propagation through bonded material becomes dominant, owing to the finite diameter of the sound field; this implies that the signal level transmitted through non-glued material in the transition region is still well below the level for glued material. Near the non-glued edges of the sample amplitude increase is observed, since some residual ultrasonic energy propagating through air is not blocked by the fixation frame (feature (4) of Fig. 2). It should be noted that the level of signals transmitted through non-glued regions is approximately 100 dB lower than the one for direct air transmission (no sample between transducers). Using a short time gate (less than 40 μs), the diffracted waves are filtered out because of their time delay with respect to signals propagating through wood.

The average voltage level measured for type B glued samples is 1 dB below the value for type A solid wood samples. This is a smaller reduction than predicted by $T_{wood,glue,wood}$ (Eq. 1) which implies higher values of $L_{glued/non-glued}$ and, therefore, further enhancement of the contrast of the ACU images. A likely reason is constructive interference of ultrasonic waves in the bonded glue line, which raises the signal level in a similar way to the non-glued case. Therefore, for practical purposes and wood species and adhesives with similar acoustic properties to the ones used in the experiments, the amplitude variations introduced by the glue line can be safely neglected with respect to other sources of variability like wood heterogeneity, which are commented below.

Effect of heterogeneity and anisotropy of wood

Wood inhomogeneity introduces variations in the voltage level measured for glued material, which should be smaller than the voltage reductions due to the presence of a non-glued area in order to ensure the detection of the latter. The heterogeneity of the inspected samples were characterised by analysing the voltage level changes in a defined scanned area of 45×150 mm ($N = 453$ points); the studied region was far enough from the edges of the lamellas to avoid boundary effects. Out of this data the coefficient of variation $CoV_{V,k}$ (%) and the maximum logarithmic variation $\Delta_{V,k}$ (dB) for each glued timber sample k were calculated:

$$CoV_{V,k} = 100\frac{s_{V,k}}{\overline{V_k}} \quad s_{V,k} = \sqrt{\frac{1}{N-1}\sum_{i=1}^{N}\left[V_k(i) - \overline{V_k}\right]^2} \quad \overline{V_k} = \frac{1}{N}\sum_{i=1}^{N}V_k(i)$$

$$\Delta_{V,k} = 20\log_{10}\frac{\max\limits_{i=1...N} V_k(i)}{\min\limits_{j=1...N} V_k(j)}$$

(3)

where $V_k(i)$ are voltage measurements for each scanned point i, and $\overline{V}_k$ and $s_{V,k}$ the mean and standard deviation of the voltage level within the scanned area. This evaluation was performed on 15 samples of type A and 18 samples of types B and C (glued material). The mean values of the coefficient of variation CoV_V (%) and maximum logarithmic variation Δ_V (dB) are shown in Table 2 for three specific time gates (see waveform in Fig. 4) and both peak and rms measurements.

Observed maximum variations were typically below 8 dB, that is, two orders of magnitude below the mean voltage level reduction measured for non-glued wood; therefore, the absence of glue can be assessed reliably down to very thin air gaps (below 100 μm). Highest variability values are obtained with longest time gates due to an increase in ultrasonic energy propagating through secondary paths (e.g. multiple reflections in the lamellas or in the damping mass of the transducers), which introduce additional sources of variation. Peak and rms measurements give similar results if the envelope of the waveform rises monotonically within the time gate. An interesting observation is that the CoV_V of a glued timber object (type B and C) is approximately half the value obtained for a solid wood sample of the same thickness (type A). From this observation it can be concluded that the variability of ultrasonic amplitude in the orthotropic T direction increases strongly with the thickness of solid wood insonified. A possible explanation is the inhomogeneity of

Table 2 Variability of ACU signal level for solid wood and glued timber

Time gate peak/rms (μs)	Samples of type A		Samples of types B and C	
	CoV_V (%)	Δ_V (dB)	CoV_V (%)	Δ_V (dB)
860–887	6.7/6.0	3.0/3.0	3.6/4.2	1.8/2.3
860–895	8.0/7.2	3.5/3.3	4.3/4.1	2.0/2.1
860–930	10.0/12.9	4.2/5.3	5.2/7.4	2.4/3.3

the speed of sound within the wood region integrated by the sound field. This may give rise to ultrasonic amplitude changes due to the interference of waves with small time of flight variations, which are larger the thicker the lamella. Another reason might be the divergence inside the sample of the ultrasonic beam with respect to the insonification axis; such variations have been previously reported for softwoods (Bucur 2002).

Some specific wood structure features could be identified comparing the ACU C-scans with photographs of the samples. Variations of the proportion of earlywood (EW) and latewood (LW) in the growth rings could be imaged in Fig. 3a, since amplitude reductions of about 5 dB are observed from highest to lowest LW concentration. A probable explanation is the fact that LW has higher acoustic impedance than EW, since $\rho_{EW} = 364 \, kg \, m^{-3}$, $c_{EW} = 1,062 \, m \, s^{-1}$, $\rho_{LW} = 636 \, kg \, m^{-3}$ and $c_{LW} = 1,468 \, m \, s^{-1}$ [speed of sound measured in the 1 MHz range, density measured with an X-ray technique; data from Bucur (2006)]. Therefore, $T_{air,LW,air} < T_{air,EW,air}$ (Eq. 1) since more acoustic energy is reflected in interfaces air-LW than in transitions air-EW. Differences of material attenuation may also have an influence on the ultrasonic level; values for the attenuation coefficients of EW and LW were not found in the literature. Neuenschwander et al. (1997) applied the variations of acoustic impedance between EW and LW to image the growth ring structure of a pine sample with 1-mm resolution; they used a water immersion reflection set-up and 2.25 MHz focused transducers. In this case, most energy was reflected in the interfaces water-EW, since the impedance mismatch is higher than in the case of water-LW.

Small material defects, such as the 26-mm-long resin pocket in Fig. 3b or small knots, decrease the measured voltage by about 3 dB. Larger defects are expected to introduce higher amplitude reductions; for example, Gan et al. (2005) have reported variations of amplitudes larger than 20 dB when imaging $40 \times 40 \, mm^2$ knots in a 34 mm thick pine block; they used a 500 kHz transducer with a spot size smaller than 1 mm. It was not possible to correlate variations of the ring angle with voltage amplitude changes in a clear fashion, an indication that the influence of anisotropy is not large for the inspected objects. Additional amplitude variation patterns of similar orders of magnitude as the ones described were observed, which could not be associated definitively to any feature of the lamellas. They might be related to the interaction of ultrasonic waves with the growth ring structure, since the wavelength of the ultrasonic pulses (about 10 mm) is similar to the year ring spacing. Feeney et al. (1997) have observed that the growth ring structure of softwoods behaves like a periodically layered composite leading to a complex frequency-dependent propagation behaviour for longitudinal waves in the orthotropic R direction. Bucur and Bohnke (1994) have reported similar observations for beech in the T direction.

Reproducibility of ACU experiments

The repeatability of ACU glued timber measurements was evaluated by measuring the same sample twice and analysing the voltage variations between the obtained C-scans. Again a $45 \times 150 \, mm^2$ glued region was insonified ($N = 453$ scanned points). Three specific scenarios were considered: (1) immediate repetition of the

measurement without removing the sample from the fixation frame, (2) repetition after 1 h, removing the sample from the frame between measurements, (3) repetition after 1 year, reinstalling all elements of the measurement set-up. A repeatability estimator $\text{Rpt}_k(x, y)$ (%) was defined as the normalised percentage difference of two C-scans $V_{2,k}(x, y)$ and $V_{1,k}(x, y)$ for the same glued timber sample k:

$$\text{Rpt}_k(x, y)(\%) = 100 \left[\frac{V_{2,k}(x, y)}{\overline{V_{2,k}}} - \frac{V_{1,k}(x, y)}{\overline{V_{1,k}}} \right] \tag{4}$$

The normalisation to the average value of each C-scan helps to compensate for gain variations in the equipment, especially in scenario (3), ensuring moreover a zero-mean estimator. The repeatability estimator can be either understood as an ultrasonic C-scan or as a set of N realisations of the random repeatability error, from which statistics such as the standard deviation $s_{\text{Rpt},k}$ (%) and maximum absolute error $\Delta_{\text{Rpt},k}$ (%) can be defined:

$$s_{\text{Rpt},k} = \sqrt{\frac{1}{N-1} \sum_{i=1}^{N} \text{Rpt}_k(i)^2}$$
$$\Delta_{\text{Rpt},k} = \max_{i=1...N} |\text{Rpt}_k(i)| \tag{5}$$

Figure 5 shows two typical reproducibility measurements for scenarios (2) and (3), together with their repeatability estimators represented as both C-scans and histograms of repeatability error. Table 3 contains averaged repeatability statistics s_{Rpt} and Δ_{Rpt} for three glued timber samples. The results are compared with the coefficient of variation $CoV_{V,\text{air}}$ (%) and maximum percentage variation

$$\Delta_{V,\text{air}} (\%) = 100 \frac{\max\limits_{i=1...N} V_{\text{air}}(i) - \min\limits_{j=1...N} V_{\text{air}}(j)}{\overline{V_{\text{air}}}} \tag{6}$$

of a set of $N = 453$ measurement points $V_{\text{air}}(i)$ obtained with direct air transmission. Peak voltage measurements with a time gate of 887–895 µs were used in all cases; the results were very similar for other time gates.

The repeatability error was found to be very low in all scenarios. In the case of scenarios 1 and 2, the repeatability C-scans present a random behaviour; no features of the originating ultrasonic images can be recognised (Fig. 5a). The repeatability error is symmetrically distributed with respect to its zero mean and fits nicely to a Gaussian distribution with a standard deviation of 0.6%. This value is in good agreement with $CoV_{V,\text{air}}$ (%); thus, the insonification of wood does not degrade the reproducibility in a significant way with respect to direct air transmission. The main repeatability error source is the timing uncertainty introduced by the digitisation process (below 200 ns), which implies that the analog waveform is not always sampled at exactly the same time positions and that slightly different peak voltages are measured in each A-scan. By performing polynomial interpolation (order 8) at the maxima of the digitised waveforms, the repeatability error was reduced by a factor of 2 (Table 2). The remaining repeatability error (less than 0.2%) might be associated with small gain drifts in the equipment, errors in the interpolation and
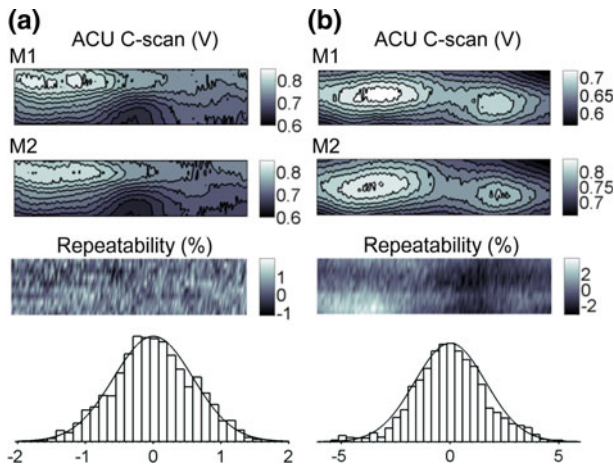
Fig. 5 Reproducibility of ACU measurements. M1 and M2 are two C-scans recorded through glued timber with a time interval between measurements of **a** 1 h and **b** 1 year. C-scans and histograms of repeatability are shown together with fitting curves corresponding to a Gaussian distribution

Table 3 Repeatability of ACU glued timber measurements	Peak interpolation without/with	s_{Rpt} (%)	Δ_{Rpt} (%)
	Immediate repetition	0.6/0.2	1.6/0.7
	1-h interval	0.6/0.3	2.1/1.3
	1-year interval	1.4/1.3	4.9/4.3
		$CoV_{V,air}$ (%)	$\Delta_{V,air}$ (%)
	Direct air signal	0.5/0.3	2.5/1.4

variations of the attenuation coefficient and acoustic impedance of air due to turbulences caused by the scanning system (Gudra 2008).

Scenario 2 shows slightly worse reproducibility than Scenario 1, which might be due to small misalignment variations between the surface of the sample and the insonification axis. Their magnitude was estimated by imaging and analysing the time of flight variations of the first reflection between receiver transducer and sample surface (feature (3) of Fig. 2). The variations were smaller than 0.15°.

The repeatability error of scenario 3 is five times larger than the value for scenarios 1 and 2, with a typical deviation of 1.3% and still a very good fitting to a normal distribution. Some patterns can be observed in the repeatability C-scans (Fig. 5b), less random than the ones of Fig. 5a. The main sources of error are thought to be larger misalignment variations between transducers or between glued timber samples and transducers (smaller than 0.4°), and small changes in moisture content of the glued timber object (the samples were conditioned to normalised climatic conditions before both measurements).

Conclusion

It was demonstrated that air-coupled ultrasound is a well-suited method to image presence and absence of adhesive in glued timber objects. Commercially available transducers plus moderate pulser voltage and receiver gain allow transmission through 10-mm-thick glued timber samples with a signal-to-noise ratio of 60 dB; therefore, inspection of thicker objects is promising. The repeatability error of two consecutive ACU amplitude measurements was as low as 0.2%, two orders of magnitude smaller than the one achieved with traditional contact techniques. In fact, in the ACU case, most uncertainties are introduced by the electrical equipment. Even repetition of ACU measurements after 1 year showed variations below 1.5% for an angular tolerance of 0.4° in the alignment between sample and transducers. This high reproducibility together with unlimited scanning possibilities illustrate the high potential of ACU, not only for industrial bonding quality assessment but also as an accurate research tool for investigating wood structure and defects. For example, the ultrasonic amplitude variations for air gaps of different thicknesses between non-glued lamellas was measured precisely for the first time (down to a level of −50 dB with respect to glued lamellas); also the mean amplitude variations between solid wood and glued wood of the same thickness (1 dB) were accurately characterised. Non-glued material was detected in all samples inspected, with a minimum air gap measured optically to be below 100 μm. Near the transition between glued and non-glued material, very thin air gaps are expected but still the voltage transmitted through non-glued wood was significantly lower than in the bonded region, which allowed for precise imaging of the transition profile. The uncertainty of ultrasonic amplitude (variations below 8 dB) in defect-free solid wood was found to be strongly related to variations of the concentration of EW and LW in the growth rings and did not compromise the detectability of non-glued regions in any case.

Future research work is planned to inspect thicker (over 10 cm) multilayered glued timber beams. The main challenge is to distinguish signal variations between bonded and disbonded areas from those due to wood heterogeneity within the bonded material (due to e.g. large wood defects or propagation through a set of thick lamellas with different acoustic properties). More involved measurement set-ups and data evaluation strategies will be used to address these issues.

References

Aicher S, Dill-Langer G, Ringger T (2002) Non-destructive detection of longitudinal cracks in glulam beams. Otto Graf J 13:165–181

Biernacki JM, Beall FC (1996) Acoustic monitoring of cold-setting adhesive curing in wood laminates. Int J Adhes Adhes 16(3):165–172

Brekhovskikh LM (1980) Waves in layered media. Academic Press, New York

Bucur V (2002) Propagation and polarization of ultrasonic waves in wood. In: Proc. of the 11th international symposium on nondestructive characterization of materials, Berlin, Germany, pp 55–60

Bucur V (2006) Acoustics of wood. Springer, Berlin

Bucur V, Bohnke I (1994) Factors affecting ultrasonic measurements in solid wood. Ultrasonics 32(5):385–390

Choi MY, Park JH, Kim WT, Kang KS (2008) Detection of delamination defect inside timber by sonic IR. In: Proc. of the society of photo-optical instrumentation engineers (SPIE), Orlando, FL, USA, pp U306–U309

Deutsch V, Platte M, Vogt M, Verein Deutscher Ingenieure (1997) Ultraschallprüfung Grundlagen und industrielle Anwendungen. Springer, Berlin

Dill-Langer G, Bernauer W, Aicher S (2005a) Inspection of glue-lines of glued-laminated timber by means of ultrasonic testing. In: Proc. of the 14th international symposium on nondestructive testing of wood, Eberswalde, Germany, pp 49–60

Dill-Langer G, Aicher S, Bernauer W (2005b) Reflection measurements at timber glue-lines by means of ultrasound shear waves. Otto Graf J 16:273–283

Dunky M, Niemz P (2002) Holzwerkstoffe und Leime: Technologie und Einflussfaktoren. Springer, Berlin

EN 14080:2005 Timber structures—glued laminated timber—requirements

EN 391:2001 Glued laminated timber—delamination test of glue lines

Feeney FE, Chivers RC, Evertsen JA, Keating J (1997) The influence of inhomogeneity on the propagation of ultrasound in wood. In: Proc. of the 17th ultrasonics international conference (UI 97), Delft, Netherlands, pp 449–453

Gan TH, Hutchins DA, Green RJ, Andrews MK, Harris PD (2005) Noncontact, high-resolution ultrasonic imaging of wood samples using coded chirp waveforms. IEEE T Ultrason Ferr 52(2):280–288

Gattiker F, Umbrecht F, Neuenschwander J, Sennhauser U, Hierold C (2007) Novel ultrasound read-out for a wireless implantable passive strain sensor (WIPSS). Sensor Actuat A-Phys 145(Sp. Iss.):291–298

Gudra T (2008) Ultrasounds in gas media: generation, transmission, applications (review paper). Arch Acoust 33(4):581–592

Hasenstab A (2006) Integritaetspruefung von Holz mit dem zerstoerungsfreien Ultraschallechoverfahren. Dissertation, Technische Universitaet Berlin

Hasenstab A, Krause M, Hillger W, Buehling L, Ilse D, Hillemeier B, Rieck C (2005) Luftultraschall und Ultraschall-Echo-Technik an Holz. In: Proc. of the German society for nondestructive testing (DGZfP), Rostock, Germany

Hu LJ, Gagnon S (2007) X-Ray-based scanning technique for non-destructive evaluation of finger-joint strength. In: Proc. of the 15th international symposium on NDT of wood, Deluth, MN, USA

Kabir MF, Schmoldt DL, Schafer ME (2002) Time domain ultrasonic signal characterization for defects in thin unsurfaced hardwood lumber. Wood Fiber Sci 34(1):165–182

Kunkle J, Vun RY, Eischeild T, Langron M, Bhardwaj N, Bhardwaj MC (2006) Phenomenal advancements in transducers and piezoelectric composites for non-contact ultrasound and other applications. In: Proc. of the European conference on non-destructive testing (ECNDT), Berlin, Germany

Maeva E, Severina I, Bondarenko S, Chapman G, O'Neill B, Severin F, Maev RG (2004) Acoustical methods for the investigation of adhesively bonded structures: a review. Can J Phys 82(12):981–1025

Neuenschwander J, Niemz P, Kucera LJ (1997) Studies for visualizing wood defects using ultrasonic techniques in reflection and transmission mode. Holz Roh- Werkst 55(5):339–340

Niemz P, Sander D (1990) Prozessmesstechnik in der Holzindustrie. VEB Fachbuchverlag, Leipzig

Rangarajan R, Krishnamurthy CV, Balasubramaniam K (2008) Ultrasonic imaging using a computed point spread function. IEEE T Ultrason Ferr 55(2):451–464

Schmerr LW, Song S-J (2007) Ultrasonic nondestructive evaluation systems models and measurements. Springer, New York

Siddiolo AM, D'Acquisto L, Maeva AR, Maev RG (2007) Wooden panel paintings investigation: an air-coupled ultrasonic imaging approach. IEEE T Ultrason Ferr 54(4):836–846

Solodov I, Pfleiderer K, Busse G (2004) Nondestructive characterization of wood by monitoring of local elastic anisotropy and dynamic nonlinearity. Holzforschung 58(5):504–510

Stoessel R (2004) Air-coupled ultrasound inspection as a new non-destructive testing tool for quality assurance. Dissertation, Universitaet Stuttgart

Vun RY, Wu QL, Bhardwaj MC, Stead G (2003) Ultrasonic characterization of structural properties of
    oriented strandboard: a comparison of direct-contact and non-contact methods. Wood Fiber Sci
    35(3):381–396